Eur. Phys. J. Plus (2022) 137:634
https://doi.org/10.1140/epjp/s13360-022-02846-w

THE EUROPEAN PHYSICAL JOURNAL PLUS

Regular Article

Testing the Einstein-Æther gravity: particle dynamics and gravitational lensing

Farruh Atamurotov[1,2,3,4,a], **Mirzabek Alloqulov**[3,5,b], **Ahmadjon Abdujabbarov**[3,5,6,7,c], **Bobomurat Ahmedov**[3,5,8,d]

[1] Inha University in Tashkent, Ziyolilar 9, 100170 Tashkent, Uzbekistan
[2] Akfa University, Milliy Bog' Street 264, 111221 Tashkent, Uzbekistan
[3] National University of Uzbekistan, 100174 Tashkent, Uzbekistan
[4] Department of Physics, Zhejiang Normal University, Jinhua 321004, China
[5] Ulugh Beg Astronomical Institute, Astronomy Street 33, 100052 Tashkent, Uzbekistan
[6] Shanghai Astronomical Observatory, 80 Nandan Road, Shanghai 200030, China
[7] Institute of Nuclear Physics, Ulugbek Street, 100214 Tashkent, Uzbekistan
[8] Tashkent Institute of Irrigation and Agricultural Mechanization Engineers, Kori Niyoziy 39, 100000 Tashkent, Uzbekistan

Received: 15 April 2022 / Accepted: 16 May 2022

Abstract The optical and energetic properties of the black hole (BH) in the Einstein-Æther gravity are investigated. In the first part of the paper, the motion of massive and massless particles including effective potential is studied under the influence of parameters of Einstein-Æther gravity. We have obtained the horizon structure, photon orbits and Innermost Stable Circular Orbit (ISCO) radius of mass particles around the BH in Einstein-Æther theory. It is shown that with the increase in the Æther parameter c_{14}, the orbits approach the central compact object, while the effect of the Æther parameter c_{13} is opposite and moves the ISCO outwards. In the second part, gravitational weak lensing is studied in more detail using the general method and the deflection angle of light rays around the black hole in plasma environment is derived. The magnification of image brightness is obtained using the angle of deflection of the light rays. Finally, we explored energy extracted from BH in Einstein-Æther gravity using the BSW (Banados–Silk–West) effect we have got expression of centre mass energy.

1 Introduction

General relativity (GR) is the standard theory of gravity, which is proposed by Einstein in 1915 and has been successfully tested using different experiments and observations. Particularly, if solar system tests [1] of GR can be considered as a test in weak field regime, then recent observation of gravitational waves [2] and shadow of M87 [3,4] can be considered as a test of GR in strong field regime. However, GR has few limitations in sense of describing the nature of the singularity during the gravitational collapse, cosmic acceleration, rotation curve of galaxies, incompatibility of GR with quantum field theory, etc. In order to resolve these problems, one needs to either break the symmetries of GR or introduce modifications or alternative theories of gravity. Indeed, there are few experimental and theoretical studies of Lorentz symmetry violations [5–7].

Among the different modifications and extensions of GR built on symmetry breaks, the Einstein-Æther theory became attractive for theoretical studies. Particularly, Einstein-Æther theory has been constructed in a such a way that Lorentz symmetry breaks down in microscale within the four-dimensional spacetime. In the action describing the spacetime together with the standard Hilbert term, there is extra additional term constructed using a unit timelike vector field. This unit vector assigns all timelike vectors of arbitrary direction and is called Æther field. The Lorentz symmetry is violated due to this Lagrangian containing Æther field and constructed using derivatives of Æther field with respect to four parameters. For given combinations of these parameters, one may obtain exact solutions of field equations describing the gravitating objects with additional parameters in the Einstein-Æther gravity. Particularly, in Ref. [8] the authors have obtained two exact solutions describing the static and electrically charged black holes within Einstein-Æther gravity using two parameters of Æther field. Numerical solutions of the field equations in the Einstein-Æther gravity have been obtained in [9].

The shadow of black hole described by the Einstein-Æther theory has been studied in [10], and authors have obtained constraints on the Æther parameter using data from Event Horizon Telescope on image of M87 [11]. Another constraint on parameters of Æther field has been obtained by analysing the data from gravitational wave observation [12]. Innermost stable circular orbits of test particles, periodic orbits and quasiperiodic oscillations have been extensively studied in [13]. In [13], authors have also explored

[a] e-mail: atamurotov@yahoo.com (corresponding author)
[b] e-mail: malloqulov@gmail.com
[c] e-mail: ahmadjon@astrin.uz
[d] e-mail: ahmedov@astrin.uz

Published online: 28 May 2022

astrophysical applications of their toy model using few known microquasars. In [14], authors have studied magnetized particle motion around black hole immersed in external magnetic field within Einstein-Æther theory.

Light bending in the vicinity of the compact gravitating object is one of the main consequences of the metric theories of gravity. The effect of gravitational lensing is responsible for the deflection of the photon from straight line. In fact, the first pioneering verification of Einstein's general relativity during the observation of solar eclipse in 1919 [15] was related to the gravitational lensing by Sun. Gravitational lensing is extensively discussed from theoretical point of view in the recent literature (see, e.g. [16–24]). The numerous works devoted to study the photon motion around compact objects, and effect of gravitational lensing can be found, for example, in Refs. [25–34] including the study of gravitational lensing in the presence of plasma in Refs. [35–51]. It is worth noting that shadow of black hole is formed by photon motion around black holes [52]. The detailed study of shadow of various black holes can be found, for example, in Refs. [53–73].

The treatment of particles' motion in environment of compact gravitating objects is powerful tool to test the spacetime properties in the strong gravitational field regime (see [74–77]). The particles orbits and their motion are very sensitive to the parameters of the gravitational field [78–84]. Thus study of test (mass) particles leads to study the parameters of field and consequently to study the theory of gravity in strong field regime. And also study of the energy extracted from a black hole is quite extended for various spacetime metrics by several authors in Refs. [85–91].

In this paper, we plan to study the test particle dynamics and gravitational lensing in the vicinity of black hole in Einstein-Æther gravity. Particularly, we plan to investigate the photon motion and gravitational lensing in the presence of plasma around black hole with nonzero Æther parameter. The work is arranged as follows: In Sect. 2, we study the properties of Einstein-Æther gravity and corresponding black hole solutions. Particle motion around BH in the Einstein-Æther gravity is investigated in Sect. 3. In Sect. 4, gravitational weak lensing is studied for various distributions of plasma around Einstein-Æther BH. Image source magnification in the presence of uniform and non-uniform plasma is explored in Sect. 5. We have also discussed the energy extraction process from the Einstein-Æther BH in Sect. 6. Section 7 is devoted to analysis of the obtained results. We use the geometrical system of units where $G = 1 = c$. Latin (Greek) indices run from 1(0) to 3.

2 Black hole in Einstein-Æther gravity

The action of Einstein-Æther theory contains the Einstein–Hilbert action with an additional term corresponding to a dynamical, unit time-like Æther field [92–94], which cannot vanish anywhere, and breaks local Lorentz symmetry. The complete action has the following form:

$$S_{æ} = \frac{1}{16\pi G_{æ}} \int d^4x\sqrt{-g}\,(R + \mathcal{L}_{æ})\,, \tag{1}$$

where $g = |g_{\mu\nu}|$ is the determinant of the metric tensor of spacetime described by the Einstein-Æther gravity. The Lagrangian of Æther field in the action (1) has the following form:

$$\mathcal{L}_{æ} = -M^{\alpha\beta}{}_{\mu\nu}(D_\alpha u^\mu)(D_\beta u^\nu) + \lambda(g_{\mu\nu}u^\mu u^\nu + 1), \tag{2}$$

here D_α is the covariant derivative with respect to x^α, λ is the Lagrangian multiplier which is responsible for the timelike Æther four-velocity u^α, and $M^{\alpha\beta}{}_{\mu\nu}$ is defined as

$$M^{\alpha\beta}{}_{\mu\nu} = c_1 g_{\mu\nu}g^{\alpha\beta} + c_2\delta^\alpha_\mu\delta^\beta_\nu + c_3\delta^\alpha_\nu\delta^\beta_\mu - c_4 u^\alpha u^\beta g_{\mu\nu}, \tag{3}$$

where c_i $(i = 1, 2, 3, 4)$ are dimensionless coupling constants introduced in this theory. Æther gravitational constant has the following form:

$$G_{æ} = \frac{G_N}{1 - \frac{1}{2}c_{14}}, \tag{4}$$

where G_N is the Newtonian gravitational constant.

The exact solution of field equations in the Einstein-Æther theory (1) describing the spacetime of spherically symmetric black hole has the following form in the spherical polar coordinates [95]:

$$ds^2 = -f(r)dt^2 + \frac{dr^2}{f(r)} + r^2(d\theta^2 + \sin^2\theta d\phi^2), \tag{5}$$

with

$$f(r) = 1 - \frac{2M}{r}\left(1 + \frac{2c_{13} - c_{14}}{4(1 - c_{13})}\frac{M}{r}\right), \tag{6}$$

and $c_{13} = c_1 + c_3$ and $c_{14} = c_1 + c_4$ are the coupling constants of the Einstein-Æther theory.

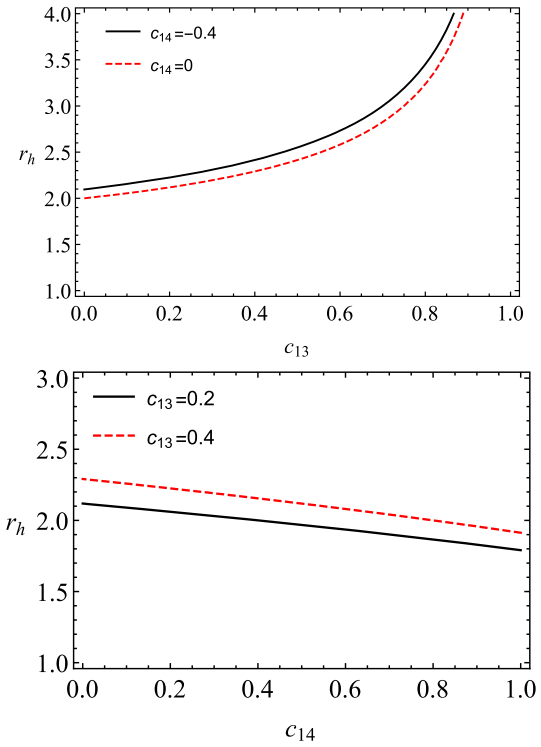

Fig. 1 Dependence of the event horizon radius r_h on parameters c_{13} and c_{14} for BH in Einstein-Æther gravity. We set $M = 1$

Now we study horizon structure of BH in Einstein-Æther gravity using $f(r) = 0$ and easily get event horizon of BH which is represented in Fig. 1. We explored different values of the parameters c_{13} and c_{14} in Einstein-Æther theory and observed that as the parameter c_{13} increases, the event horizon is increased and, in opposite interestingly, as the parameter c_{14} increases, the event horizon is decreased.

3 Particle dynamics around black hole in Einstein-Æther gravity

In this section, we investigate the motion of massive and massless particles around a black hole in Einstein-Æther gravity.

3.1 Massive particles motion around black hole in Einstein-Æther gravity

First we study massive particle motion around the regular black hole in Einstein-Æther gravity. In order to find the trajectory of the test particle, one needs to consider Lagrangian for the test particle of mass m of the following form

$$L' = \frac{1}{2} g_{\mu\nu} u^\mu u^\nu, \qquad u^\mu = \frac{dx^\mu}{d\tau}, \tag{7}$$

where τ is an affine parameter, x^μ and u^μ are the coordinates and four-velocity of the test particle, respectively. The conservative quantities of the motion such as the energy $\mathcal{E}$ and the angular momentum $\mathcal{L}$ of the test particle can be written in the following form:

$$\begin{aligned} \mathcal{E} &= \frac{\partial L'}{\partial u^t} = -f(r)\frac{dt}{d\tau}, \\ \mathcal{L} &= \frac{\partial L'}{\partial u^\phi} = r^2 \sin^2\theta \frac{d\phi}{d\tau}. \end{aligned} \tag{8}$$

By inserting expressions in (8) into the normalization condition $g_{\mu\nu} u^\mu u^\nu = -\epsilon$, one can easily find the equations of motion of test particle in the following form:

$$\frac{\mathrm{d}r}{\mathrm{d}\tau} = \sqrt{\mathcal{E}^2 - f(r)\left(\epsilon + \frac{\mathcal{K}}{r^2}\right)}, \tag{9}$$

$$\frac{\mathrm{d}\theta}{\mathrm{d}\tau} = \frac{1}{r^2}\sqrt{\mathcal{K} - \frac{\mathcal{L}^2}{\sin^2\theta}}, \tag{10}$$

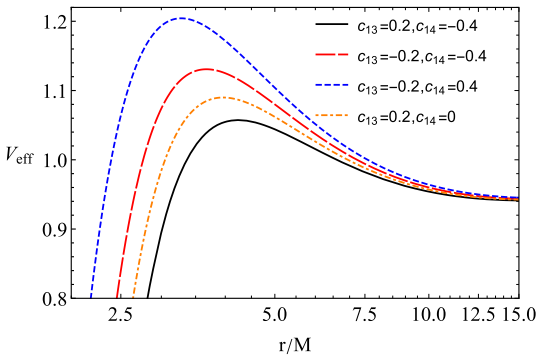

Fig. 2 Dependence of V_{eff} on radial coordinate r of massive particle for the different values of Einstein-Æther BH parameters c_{13} and c_{14}

$$\frac{\mathrm{d}\phi}{\mathrm{d}\tau} = \frac{\mathcal{L}^2}{r^2 \sin^2\theta}, \tag{11}$$

$$\frac{\mathrm{d}t}{\mathrm{d}\tau} = \frac{\mathcal{E}}{f(r)}, \tag{12}$$

where $\mathcal{K}$ is the Carter constant and the parameter ϵ is defined as:

$$\epsilon = \begin{cases} 1, & \text{for timelike geodesics} \\ 0, & \text{for null geodesics} \\ -1, & \text{for spacelike geodesics.} \end{cases} \tag{13}$$

For simplicity, one can consider the motion of the particles in the equatorial plane in which $\theta = \frac{\pi}{2}$ and $\frac{d\theta}{d\tau} = 0$. In this special case, Carter constant takes form $\mathcal{K} = \mathcal{L}^2$ and the equation for the radial motion takes the following form:

$$\left(\frac{dr}{d\tau}\right)^2 = \mathcal{E}^2 - V_{eff}(r) = \mathcal{E}^2 - f(r)\left(1 + \frac{\mathcal{L}^2}{r^2}\right), \tag{14}$$

with

$$V_{eff} = f(r)(1 + \frac{\mathcal{L}^2}{r^2}), \tag{15}$$

being the effective potential of the radial motion of test particles. The radial dependence of the effective potential for the massive test particle around BH in Einstein-Æther theory for different values of c_{13} and c_{14} parameters is represented in Fig. 2. It can be seen from the graphs that under the influence of the c_{13} parameter the stable circular orbits move towards the central compact object and the effect of the c_{14} parameter has an opposite behaviour, i.e. the stable circular orbits move outwards the central compact object.

In order to derive the circular motion of the neutral particle around BH, one can use the following conditions $\dot{r} = 0$ and $\ddot{r} = 0$. These conditions allow one to obtain expressions for the energy $\mathcal{E}$ and the angular momentum $\mathcal{L}$ of the test particle in the following form

$$\mathcal{L}^2 = \frac{Mr^2(M(c_{14} - 2c_{13}) + 2(c_{13} - 1)r)}{2M^2(2c_{13} - c_{14}) - 6(c_{13} - 1)Mr + 2(c_{13} - 1)r^2}, \tag{16}$$

and

$$\mathcal{E}^2 = \frac{\left(-2c_{13}(M - r)^2 + c_{14}M^2 + 2r(r - 2M)\right)^2}{4(c_{13} - 1)r^2\left(M^2(2c_{13} - c_{14}) - 3(c_{13} - 1)Mr + (c_{13} - 1)r^2\right)}. \tag{17}$$

In order to get more information about conservative quantities, one can make plot for them, and it is shown in Fig. 3. The graphs indicate that under the influence of the c_{13} parameter the radial coordinates are shifted towards the centre, and conversely, the effect of the c_{14} parameter shifts the radial coordinates outwards direction.

Now we may consider the inner stable circular orbit r_{ISCO}. In order to find ISCO radius, one needs to use the following conditions:

$$\begin{cases} V'_{\text{eff}} = 0 \\ V''_{\text{eff}} = 0. \end{cases} \tag{18}$$

Due to the complex form of the effective potential, we cannot get exact analytical expression of r_{ISCO}. However, one may represent the radius of ISCO using the graphs, and it is represented for various parameters c_{13} and c_{14} in Fig. 4. From this, one can get

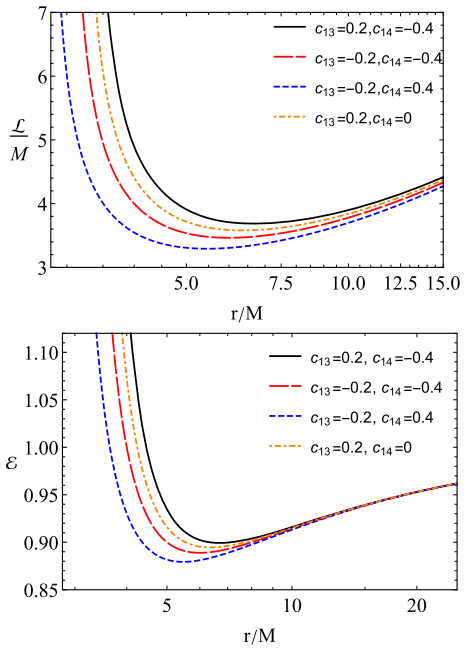

Fig. 3 Radial dependence of $\mathcal{L}$ and $\mathcal{E}$ for the different values of Æther parameters

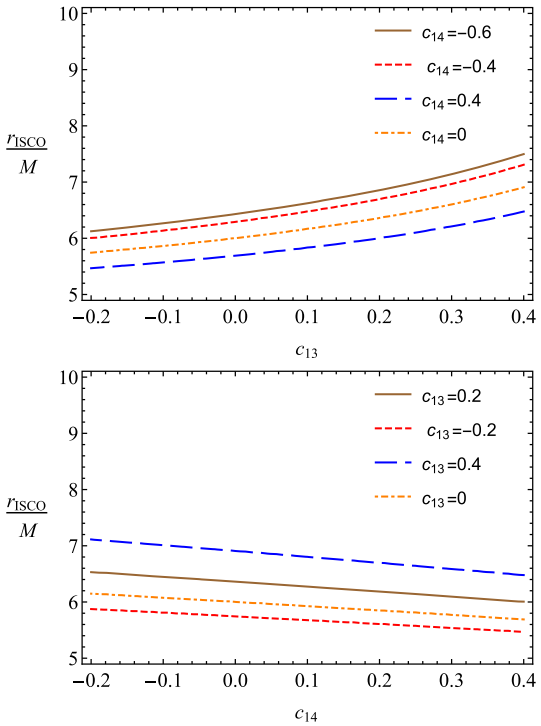

Fig. 4 Relation of r_{ISCO}/M on parameters c_{13} and c_{14} in Einstein-Æther gravity

information about inner stable circular orbits dependence on parameter c_{13} and c_{14} in Einstein-Æther gravity. Particularly, ISCO radius increases with the increase in parameter c_{13}. ISCO radius decreases with the increase in parameter c_{14} in Fig. 4.

3.2 Massless particle (photon) motion

In this subsection, we explore massless particle (photon) motion in spacetime of BH in Einstein-Æther gravity. Using Lagrangian (7), equation of photon motion around compact object can be obtained by setting $\epsilon = 0$ (13) and at the equatorial plane can be expressed in the following form:

$$\dot{r}^2 = \mathcal{E}^2 - f(r)\frac{\mathcal{L}^2}{r^2}, \tag{19}$$

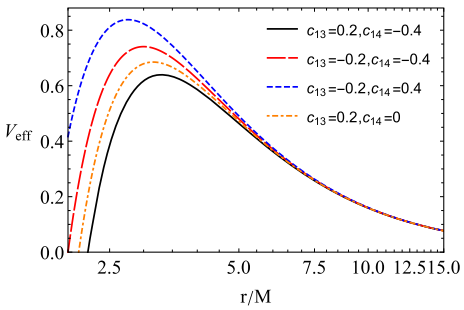

Fig. 5 Dependence of $V_{\rm eff}$ on radial coordinate r of photon for the different values of Einstein-Æther BH parameters c_{13} and c_{14}

$$\dot{\phi} = \frac{\mathcal{L}}{r^2}, \tag{20}$$

$$\dot{t} = \frac{\mathcal{E}}{f(r)}. \tag{21}$$

Using Eq. (19), one can easily get expression of effective potential V_{eff} for the radial motion of photon as

$$V_{eff} = f(r)\frac{\mathcal{L}^2}{r^2}. \tag{22}$$

The radial dependence of effective potential for radial motion of photons is shown in Fig. 5. From this figure, one can easily see that photon orbits shift towards the central BH under the effect of the c_{13} parameter and vice versa of the c_{14} parameter.

Radius of photon's circular orbit r_{ph} around BH in Einstein-Æther gravity can be found as solution of the following equation:

$$V'_{eff} = 0,$$

which leads to the following solution

$$r_{ph} = \frac{-\sqrt{c_{13}^2M^2 - 10c_{13}M^2 + 4c_{13}c_{14}M^2 - 4c_{14}M^2 + 9M^2}}{2\,(c_{13}-1)} + \frac{3c_{13}M - 3M}{2\,(c_{13}-1)} \tag{23}$$

The dependence of the radius of photon orbits r_{ph} on Æther parameters c_{13} and c_{14} of Einstein-Æther gravity is shown in Fig. 6. One can see that the radius of the photon orbit is increased with the increase in the parameter c_{13}, while the effect of the parameter c_{14} on radius of photon orbits is opposite.

4 Weak gravitational lensing in Einstein-Æther gravity

In this section, we test optical properties of BH in Einstein-Æther gravity using gravitational weak lensing effect. For a weak-field approximation, one can use the following notation of metric tensor as [35,40]

$$g_{\alpha\beta} = \eta_{\alpha\beta} + h_{\alpha\beta}, \tag{24}$$

where $\eta_{\alpha\beta}$ and $h_{\alpha\beta}$ refer to the expressions for Minkowski spacetime and perturbation gravity field describing Einstein-Æther theory, respectively. One has to require the following properties for $\eta_{\alpha\beta}$ and $h_{\alpha\beta}$

$$\begin{aligned} &\eta_{\alpha\beta} = diag(-1,1,1,1),\\ &h_{\alpha\beta} \ll 1, \quad h_{\alpha\beta} \to 0 \quad under\ \ x^{\alpha} \to \infty,\\ &g^{\alpha\beta} = \eta^{\alpha\beta} - h^{\alpha\beta}, \quad h^{\alpha\beta} = h_{\alpha\beta}. \end{aligned} \tag{25}$$

Using the fundamental equation, we can get the expression for the angle of deflection around a compact object in Einstein-Æther gravity as follows [35]:

$$\hat{\alpha}_{\rm b} = \frac{1}{2}\int_{-\infty}^{\infty}\frac{b}{r}\left(\frac{{\rm d}h_{33}}{{\rm d}r} + \frac{1}{1-\omega_e^2/\omega}\frac{{\rm d}h_{00}}{{\rm d}r} - \frac{K_e}{\omega^2-\omega_e^2}\frac{{\rm d}N}{{\rm d}r}\right){\rm d}z, \tag{26}$$

where ω and ω_e are known as quantities representing the photon and plasma frequencies, respectively. One may rewrite metric element (5) in the form

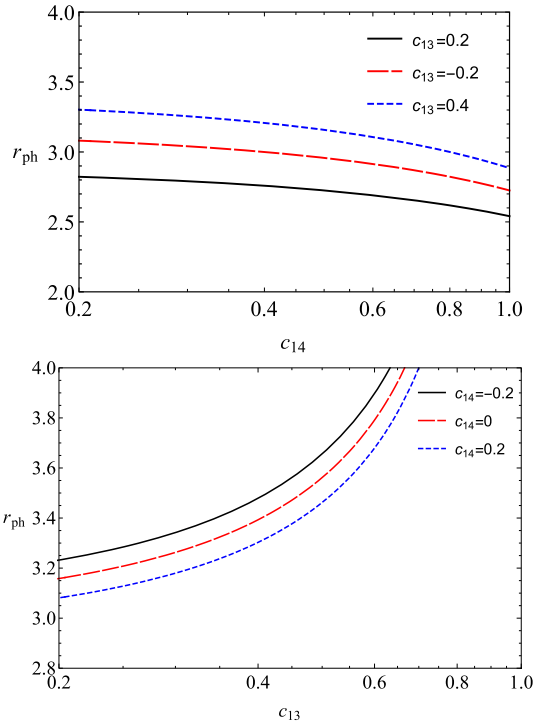

Fig. 6 Dependence of radius of photon r_{ph} on parameters c_{13} and c_{14} of Einstein-Æther gravity

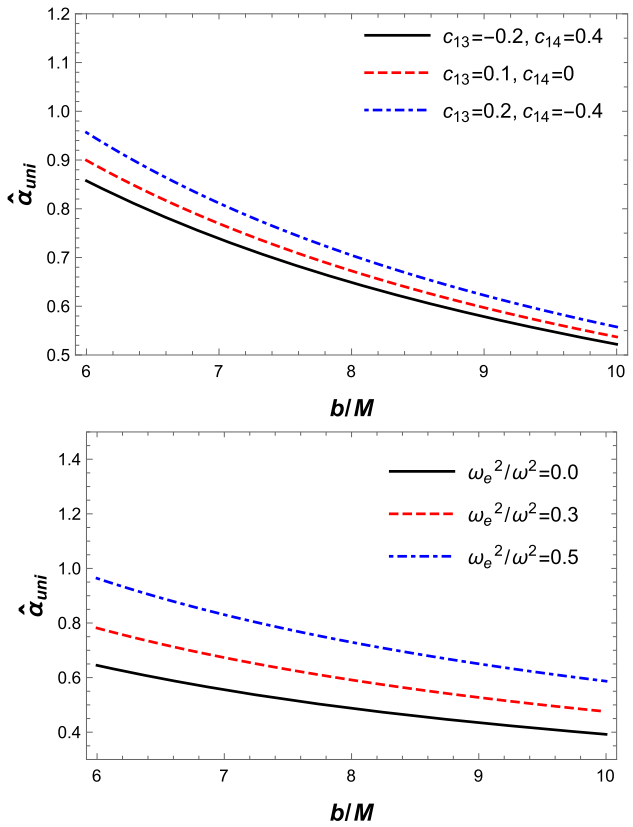

Fig. 7 The dependence of the deflection angle $\hat{\alpha}_{\text{uni}}$ on the impact parameter b for the different values of parameters c_{13} and c_{14} (upper panel) and plasma medium (lower panel)

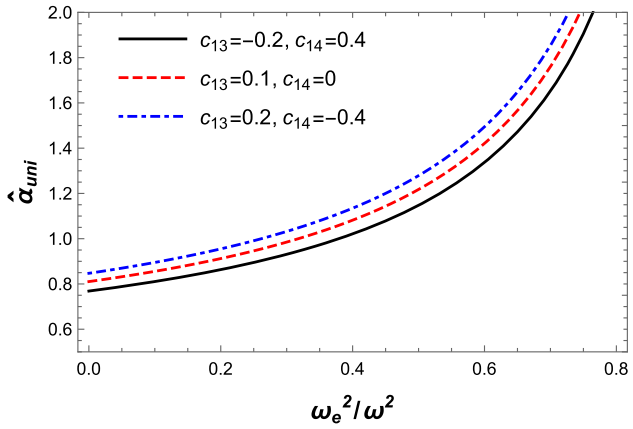

Fig. 8 The dependence of the deflection angle $\hat{\alpha}_{\rm uni}$ on plasma parameters for the fixed value of impact parameter $b = 5M$

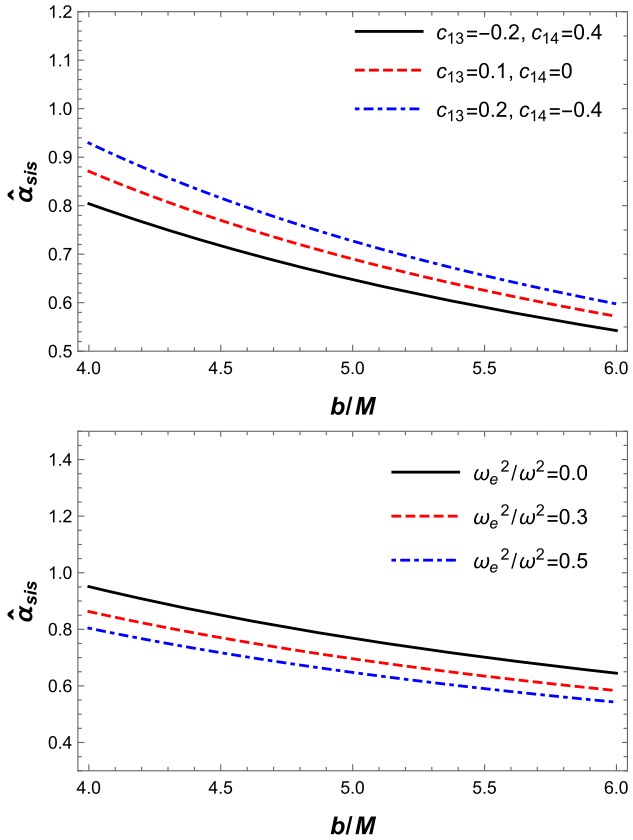

Fig. 9 The dependence of the deflection angle $\hat{\alpha}_{\rm sis}$ on the impact parameter for the different values of parameters c_{13} and c_{14} (upper panel) and plasma parameters (lower panel)

$$\begin{aligned} \mathrm{d}s^2 = \mathrm{d}s_0^2 + \frac{2M}{r}\left(1 + \frac{(2c_{13} - c_{14})M}{4(1 - c_{13})r}\right)\mathrm{d}t^2 \\ + \frac{2M}{r}\left(1 + \frac{(2c_{13} - c_{14})M}{4(1 - c_{13})r}\right)\mathrm{d}r^2, \end{aligned} \tag{27}$$

where $ds_0^2 = -dt^2 + dr^2 + r^2(d\theta^2 + \sin^2\theta d\phi^2)$.

Now one may easily find components $h_{\alpha\beta}$ of metric element in Cartesian coordinates in the form

$$h_{00} = \frac{2M}{r}\left(1 + \frac{(2c_{13} - c_{14})M}{4(1 - c_{13})r}\right) \tag{28}$$

$$h_{ik} = \left(\frac{2M}{r}\left(1 + \frac{(2c_{13} - c_{14})M}{4(1 - c_{13})r}\right)\right) n_i n_k \tag{29}$$

$$h_{33} = \frac{2M}{r}\left(1 + \frac{(2c_{13} - c_{14})M}{4(1 - c_{13})r}\right)\cos^2\chi, \tag{30}$$

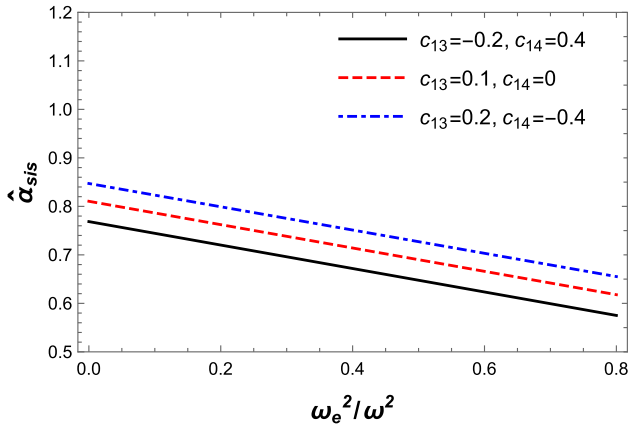

Fig. 10 The dependence of the deflection angle $\hat{\alpha}_{\rm sis}$ on plasma for the fixed value of impact parameter $b = 5M$

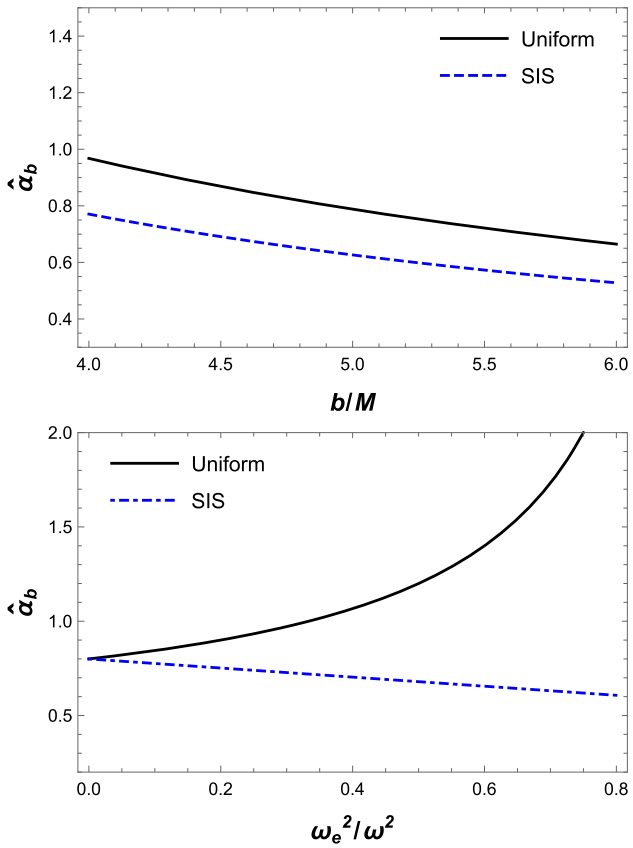

Fig. 11 The dependence of the deflection angle $\hat{\alpha}_{\rm b}$ on the impact parameter (upper panel) and the plasma parameters (lower panel)

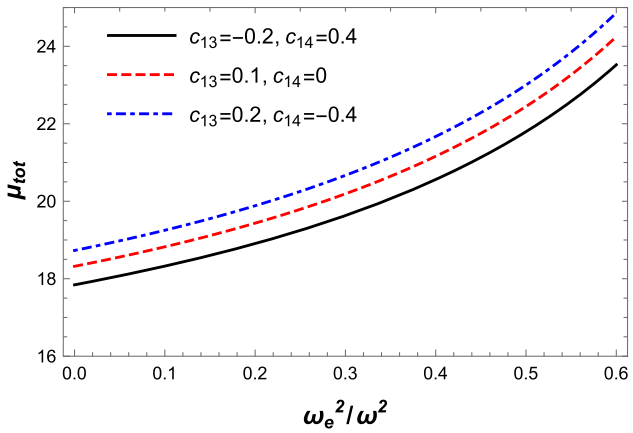

Fig. 12 The dependence of the total magnification μ_{tot} on the plasma parameter for the different values of parameter c_{13} and c_{14} corresponding to the fixed value of impact parameter $b = 5M$

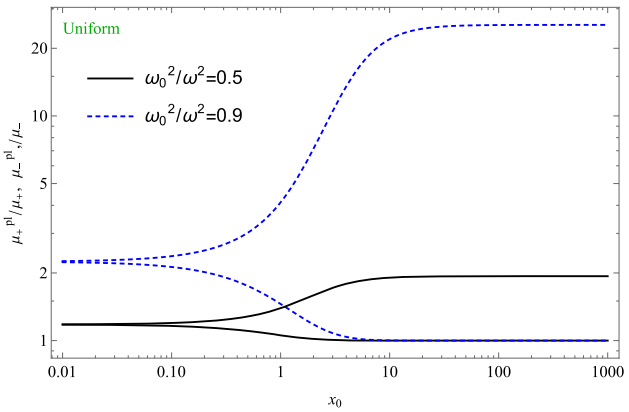

Fig. 13 Image magnification in the presence of uniform plasma. The fixed parameters used are $M = 1, b = 3M, c_{13}$=-0.2 and c_{14}=0.4

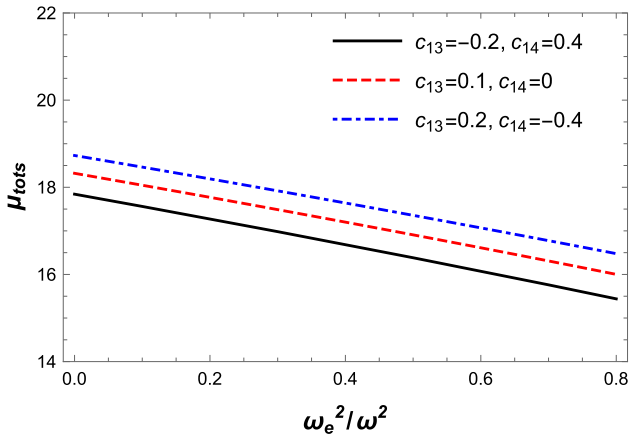

Fig. 14 The total magnification of the images as a function of non-uniform plasma. Here impact parameter is set as $b = 5M$

where $\cos^2\chi = z^2/(b^2+z^2)$ and $r^2 = b^2 + z^2$. The derivatives of h_{00} and h_{33} by radial coordinate are defined as:

$$\frac{\mathrm{d}h_{00}}{\mathrm{d}r} = -\frac{c_{14}M^2}{(c_{13}-1)r^3} + \frac{2c_{13}M^2}{(c_{13}-1)r^3} - \frac{2c_{13}M}{(c_{13}-1)r^2} + \frac{2M}{(c_{13}-1)r^2}, \tag{31}$$

$$\frac{\mathrm{d}h_{33}}{\mathrm{d}r} = -\frac{2c_{14}M^2z^2}{(c_{13}-1)r^5} + \frac{4c_{13}M^2z^2}{(c_{13}-1)r^5} - \frac{6c_{13}Mz^2}{(c_{13}-1)r^4} + \frac{6Mz^2}{(c13-1)r^4}. \tag{32}$$

We can write the following expression for the deflection angle [49]

$$\hat{\alpha_b} = \hat{\alpha_1} + \hat{\alpha_2} + \hat{\alpha_3}, \tag{33}$$

with

$$\begin{aligned}
\hat{\alpha_1} &= \frac{1}{2}\int_{-\infty}^{\infty}\frac{b}{r}\frac{\mathrm{d}h_{33}}{\mathrm{d}r}\mathrm{d}z,\\
\hat{\alpha_2} &= \frac{1}{2}\int_{-\infty}^{\infty}\frac{b}{r}\frac{1}{1-\omega_e^2/\omega}\frac{\mathrm{d}h_{00}}{\mathrm{d}r}\mathrm{d}z\,,\\
\hat{\alpha_3} &= \frac{1}{2}\int_{-\infty}^{\infty}\frac{b}{r}\left(-\frac{K_e}{\omega^2-\omega_e^2}\frac{\mathrm{d}N}{\mathrm{d}r}\right)\mathrm{d}z.
\end{aligned} \tag{34}$$

Now we plan to check and evaluate the deflection angle for different plasma density distributions.

4.1 Uniform plasma

In this subsection, gravitational deflection angle around BH in Einstein-Æther gravity in the presence of a uniform plasma can be written as sum [49]

$$\hat{\alpha}_{\mathrm{uni}} = \hat{\alpha}_{uni1} + \hat{\alpha}_{uni2} + \hat{\alpha}_{uni3}. \tag{35}$$

From Eqs. (34), (30) and (33), we may easily get the expression of deflection angle around BH in Einstein-Æther gravity in a uniform plasma medium as

$$\hat{\alpha}_{uni} = \frac{2M}{b} + \frac{\pi c_{14} M^2}{8b^2(c_{13}-1)} - \frac{\pi c_{13} M^2}{4b^2(c_{13}-1)} + \\ + \left(\frac{2M}{b} + \frac{\pi c_{14} M^2}{4b^2(c_{13}-1)} - \frac{\pi c_{13} M^2}{2b^2(c_{13}-1)}\right) \frac{\omega^2}{\omega^2 - \omega_e^2}. \tag{36}$$

Using the above equation, we plot the dependence of the angle of deflection on the impact parameter b for different values of parameters c_{13}, c_{14}, ω_e^2/ω^2 in spacetime of BH in Einstein-Æther gravity, and it is represented in Fig. 7. Also we have explored the dependence of deflection angle on plasma parameters for selected values of Einstein-Æther parameters c_{13} and c_{14} and they are presented in Fig. 8

4.2 Non-uniform plasma

In this part of our current analysis, we consider that non-singular isothermal sphere (SIS) is the most favourable model to comprehend peculiar features of gravitational weak lensed photons around BH. Generally, SIS is spherical gas cloud with a singularity located at its centre where the density tends to infinity. The density distribution of a SIS is given by [35]:

$$\rho(r) = \frac{\sigma_v^2}{2\pi r^2}, \tag{37}$$

where σ_v^2 refers to a one-dimensional velocity dispersion. The plasma concentration admits the following analytic expression [35]

$$N(r) = \frac{\rho(r)}{k m_p}, \tag{38}$$

where m_p is proton mass and k is a dimensionless constant coefficient generally associated with the dark matter universe. The plasma frequency is:

$$\omega_e^2 = K_e N(r) = \frac{K_e \sigma_v^2}{2\pi k m_p r^2}. \tag{39}$$

Now we explore non-uniform plasma (SIS) effect on deflection angle in spacetime of Einstein-Æther black hole. We may write the expression of deflection angle around BH in Einstein-Æther gravity as [49]

$$\hat{\alpha}_{\rm SIS} = \hat{\alpha}_{SIS1} + \hat{\alpha}_{SIS2} + \hat{\alpha}_{SIS3}. \tag{40}$$

Combining Eqs. (30), (34), (40), deflection angle can be written in the following form:

$$\hat{\alpha}_{SIS} = \frac{3\pi c_{14} M^2}{8b^2(c_{13}-1)} - \frac{3\pi c_{13} M^2}{4b^2(c_{13}-1)} + \frac{4M}{b} + \\ + \frac{3c_{14} k M^4}{4b^4(c_{13}-1)} - \frac{3c_{13} k M^3}{2b^4(c_{13}-1)} - \frac{4kM^2}{\pi b} + \frac{16kM^3}{3\pi b^3}. \tag{41}$$

These calculations bring up a supplementary plasma constant ω_c^2, which has the following analytic expression [40]

$$\omega_c^2 = \frac{K_e \sigma_v^2}{2\pi k m_p R_S^2}. \tag{42}$$

From Eq. (41), we do graphs for the dependence of the angle of deflection on the impact parameter b for different values of parameters c_{13}, c_{14}, ω_c^2/ω^2 for non-uniform plasma medium in Einstein-Æther spacetime, and it is shown in Fig. 9. Then, we demonstrate the dependence of the angle of deflection of a light ray around a BH in the presence of a non-uniform plasma in Figs. 9 and 10.

In addition, we compared the different effects of plasma on the Einstein-Æther BH deflection angle with gravity, as shown in Fig. 11.

5 Magnification of gravitationally lensed image

Now we explore the brightness of the image in the presence of a plasma through the deflection angle of light rays around BH in the Einstein-Æther gravity. Using the lens equation, we can write the combination of light angles around BH in Einstein-Æther gravity

($\hat{\alpha}$, θ and β) [37,40] as

$$\theta D_{\rm s} = \beta D_{\rm s} + \hat{\alpha} D_{\rm ds}, \tag{43}$$

where $D_{\rm s}$, $D_{\rm d}$ and $D_{\rm ds}$ are the distances from the source to the observer, from the lens to the observer and from the source to the lens, respectively, and θ and β refer to the angular position of the image and the source. Now, from the above equation, we can rewrite equation for β as follows:

$$\beta = \theta - \frac{D_{\rm ds}}{D_{\rm s}} \frac{\xi(\theta)}{D_{\rm d}} \frac{1}{\theta}\,, \tag{44}$$

where $\xi(\theta) = |\hat{\alpha}_b| b$ and $b = D_{\rm d}\theta$ have been used in [40]. If the shape of the image looks like a ring, it is defined as Einstein's ring and radius of Einstein's ring is $R_s = D_{\rm d}\theta_E$. The angular θ_E due to spacetime geometry between the images of the source in a vacuum [20] can be written as

$$\theta_E = \sqrt{2R_s \frac{D_{ds}}{D_d D_s}}. \tag{45}$$

Now, we explore the expression of the magnification of brightness [20]

$$\mu_\Sigma = \frac{I_{\rm tot}}{I_*} = \sum_k \left| \left(\frac{\theta_k}{\beta}\right) \left(\frac{{\rm d}\theta_k}{{\rm d}\beta}\right) \right|, \quad k = 1, 2, \ldots, j, \tag{46}$$

where I_* and $I_{\rm tot}$ are the unlensed brightness of the source and the total brightness of all images, respectively. The expressions of the magnification of the source are written in the following form [20]:

$$\mu_+^{\rm pl} = \frac{1}{4}\left(\frac{x}{\sqrt{x^2+4}} + \frac{\sqrt{x^2+4}}{x} + 2 \right), \tag{47}$$

$$\mu_-^{\rm pl} = \frac{1}{4}\left(\frac{x}{\sqrt{x^2+4}} + \frac{\sqrt{x^2+4}}{x} - 2 \right), \tag{48}$$

where $x = \beta/\theta_0$ is a dimensionless quantity [40], and $\mu_+^{\rm pl}$ and $\mu_-^{\rm pl}$ are the images. Using Eqs. (47) and (48), one can get formula for the total magnification in the following form:

$$\mu_{\rm tot}^{\rm pl} = \mu_+^{\rm pl} + \mu_-^{\rm pl} = \frac{x^2+2}{x\sqrt{x^2+4}}\,. \tag{49}$$

Now we investigate the magnification in the presence of plasma in BH environment with different distributions: (i) uniform and (ii) non-uniform cases.

5.1 Uniform Plasma

In this subsection, we explore the effect of uniform plasma on magnification of image in Einstein-Æther theory and we may write expressions for total magnification μ_{tot}^{pl} and angle $\theta_{\rm uni}^{\rm pl}$ as

$$\mu_{\rm tot}^{\rm pl} = \mu_+^{pl} + \mu_-^{pl} = \frac{x_{\rm uni}^2 + 2}{x_{\rm uni}\sqrt{x_{\rm uni}^2+4}}\,, \tag{50}$$

and

$$\theta_{\rm uni}^{\rm pl} = \theta_0 \sqrt{\frac{1}{2}\left((A+1)\frac{1}{1-\frac{\omega_0^2}{\omega^2}} + \frac{A}{2} + 1 \right)}, \tag{51}$$

with dimensionless for simplification

$$A = \frac{\pi\,(c_{14} - 2c_{13})\,M}{8b\,(c_{13}-1)}, \tag{52}$$

where $x_{\rm uni}$, $(\mu_+^{\rm pl})_{\rm uni}$ and $(\mu_-^{pl})_{uni}$ are defined as

$$x_{\rm uni} = \frac{\beta}{(\theta_E^{pl})_{\rm uni}} = \\ = \frac{x_0}{\sqrt{\frac{1}{2}\left((A+1)\frac{1}{1-\frac{\omega_0^2}{\omega^2}}+\frac{A}{2}+1\right)}} \tag{53}$$

$$(\mu_+^{\rm pl})_{\rm uni} = \frac{1}{4}\left(\frac{x_{\rm uni}}{\sqrt{x_{\rm uni}^2+4}}+\frac{\sqrt{x_{\rm uni}^2+4}}{x_{\rm uni}}+2\right) \tag{54}$$

$$(\mu_-^{pl})_{uni} = \frac{1}{4}\left(\frac{x_{\rm uni}}{\sqrt{x_{\rm uni}^2+4}}+\frac{\sqrt{x_{\rm uni}^2+4}}{x_{\rm uni}}-2\right) \tag{55}$$

The total magnification of the image in the presence of a plasma $\mu_{\rm tot}^{\rm pl}$ in Einstein-Æther gravity is represented in Fig. 12, and the total magnification is decreased with ω_e^2/ω^2 for the different values of parameters c_{13} and c_{14} in Einstein-Æther spacetime. Plot for dependence of the total magnification on x_0 in the presence of uniform plasma for fixed values of the parameters c_{13} and c_{14} is demonstrated in Fig. 13.

5.2 Non-uniform plasma

Here, we study the effect of non-uniform plasma (as SIS medium) on magnification, which can be written as:

$$(\mu_{\rm tot}^{\rm pl})_{\rm SIS} = (\mu_+^{\rm pl})_{\rm SIS} + (\mu_-^{\rm pl})_{\rm SIS} = \frac{x_{\rm SIS}^2+2}{x_{\rm SIS}\sqrt{x_{\rm SIS}^2+4}}\,, \tag{56}$$

with

$$(\mu_+^{\rm pl})_{\rm SIS} = \frac{1}{4}\left(\frac{x_{\rm SIS}}{\sqrt{x_{\rm SIS}^2+4}}+\frac{\sqrt{x_{\rm SIS}^2+4}}{x_{\rm SIS}}+2\right)\,, \tag{57}$$

$$(\mu_-^{\rm pl})_{\rm SIS} = \frac{1}{4}\left(\frac{x_{\rm SIS}}{\sqrt{x_{\rm SIS}^2+4}}+\frac{\sqrt{x_{\rm SIS}^2+4}}{x_{\rm SIS}}-2\right)\,, \tag{58}$$

and

$$x_{\rm SIS} = \frac{\beta}{(\theta_E^{\rm pl})_{\rm SIS}} \\ = \frac{x_0}{\sqrt{\frac{3\omega_c^2M^2(c_{14}M-2c_{13})}{16b^3\omega^2(c_{13}-1)}+\frac{4\omega_c^2M^2}{3\pi\omega^2b^2}-\frac{M\omega_c^2}{\pi\omega^2}+\frac{3A}{4}+1}}. \tag{59}$$

Using Eq. (56), one can find the dependence of total magnification on plasma parameter and with the increase in plasma parameter magnification is decreased, which is represented in Fig. 14. Also, the plot of dependence of total magnification on x_0 in the presence of plasma for the fixed values of the parameters c_{13} and c_{14} is presented in Fig. 15. Finally, we compare in Fig. 16 these two cases, which are for uniform and non-uniform plasma distributions.

6 Extracted energy by collisions

Now we study the particle acceleration process of two charged particles colliding near the horizon of the black hole in the Einstein-Æther gravity. We consider two particles that have rest masses m_1 and m_2 at a distance far away from BH, and we can write equations of motion as

$$p^\alpha = mu^\alpha, \tag{60}$$

$$u^t = \frac{\mathcal{E}}{f(r)}, \tag{61}$$

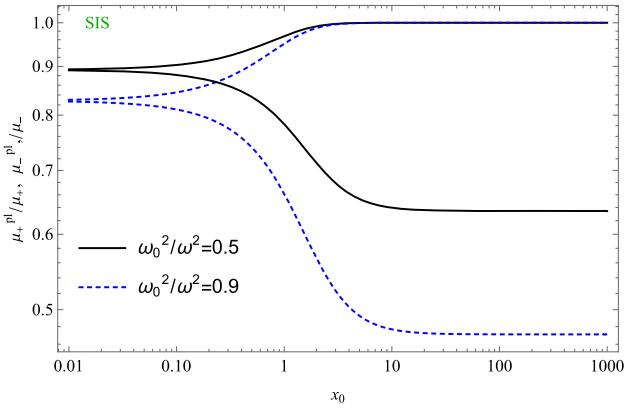

Fig. 15 Image magnification in the presence of SIS. The fixed parameters used are $M = 1$, $b = 3M$, c_{13}=-0.2 and c_{14}=0.4

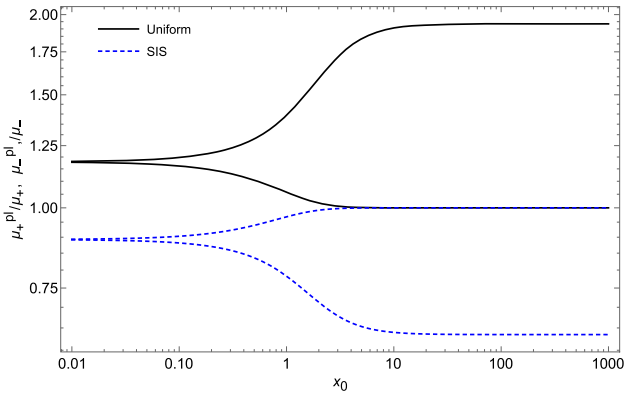

Fig. 16 Image magnifications in the presence of uniform plasma and SIS. The fixed parameters used are $M = 1$, $b = 3M$, $\frac{\omega_0^2}{\omega^2} = 0.5$, $\frac{\omega_c^2}{\omega^2} = 0.5$, c_{13}=-0.2 and c_{14}=0.4

$$u^{\phi} = \frac{\mathcal{L}}{r^2}, \tag{62}$$

$$u^{r} = \sqrt{\mathcal{E}^2 - f(r)\left(1 + \frac{\mathcal{L}^2}{r^2}\right)}. \tag{63}$$

The extracted energy $E_{C.M.}$ by collision between two particles is defined by [74]

$$\frac{E_{C.M.}}{2m_1m_2} = \frac{m_1^2 + m_2^2}{2m_1m_2} - g_{\alpha\beta}u_1^{\alpha}u_2^{\beta}. \tag{64}$$

By using Eqs. (61), (62) and (63), we can rewrite Eq. (64) for the energy extracted as

$$\frac{E_{C.M.}}{2m_1m_2} = 1 + \frac{(m_1 - m_2)^2}{2m_1m_2} + \frac{\mathcal{E}_1\mathcal{E}_2}{f(r)} - \frac{\mathcal{L}_1\mathcal{L}_2}{r^2} - \frac{1}{f^2(r)}\sqrt{\mathcal{E}_1^2 - f(r)\left(1 + \frac{\mathcal{L}_1^2}{r^2}\right)}\sqrt{\mathcal{E}_2^2 - f(r)\left(1 + \frac{\mathcal{L}_2^2}{r^2}\right)}, \tag{65}$$

where $f(r)$ is the known lapse function of the gravity.

The radial dependence of $E_{C.M.}$ energy of BH can be seen in Fig. 17. From Fig. 17 (upper panel), the minimum energy shows that two particles have opposite angular momentum. This graph is drawn for $c_{13} = c_{14} = 0.2$ case. Figure 17 (lower panel) illustrates the radial dependence of centre-of-mass energy of colliding for two non-spinning particles for the different values of the Æther parameters. In this plot considered head-on collision with the specific angular momentum $\mathcal{L}_1 = -\mathcal{L}_2 = 2M$. We can see that the value of energy increases with increasing parameter c_{13} and decreasing parameter c_{14}.

7 Conclusions

In this work, we have studied the optical and energetic properties of BH in the Einstein-Æther gravity for mass and massless particles, and from this work, we can draw the following conclusions:

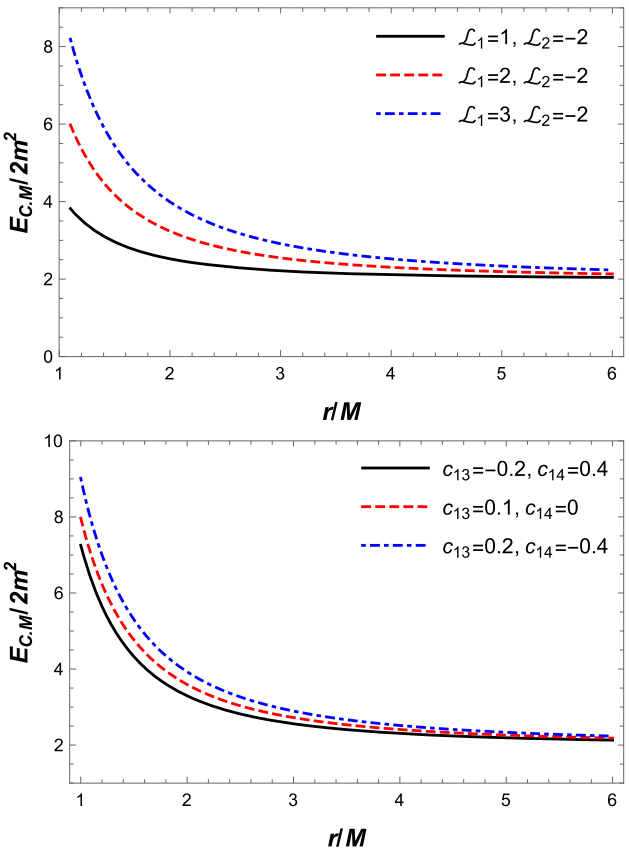

Fig. 17 The relationship of $E_{C.M}$ to radial coordinate r/M is described for different $\mathcal{L}_1$ and $\mathcal{L}_2$ values (upper panel) and for different Æther parameters(lower panel)

- We have studied the structure of the horizon of BH in the Einstein-Æther gravity. It can be seen from the obtained results that with the increase of the parameter c_{13} radius of the event horizon is increased, and for the parameter c_{14} it is vice versa as demonstrated in Fig. 1.
- For particle motion around compact object, we have discussed effective potential. We also studied the dependence of effective potential of massive and massless particles on radial coordinate for different values of the Einstein-Æther parameters c_{13} and c_{14}.
- ISCO is investigated for the massive particles around BH in the Einstein-Æther gravity including parameters c_{13} and c_{14}. It is demonstrated that with the increase in parameter c_{13} ISCO radius is slightly increased, but influence of parameter c_{14} is opposite as demonstrated in Fig. 4.
- Radius of photon sphere is explored around BH in Einstein-Æther gravity. Orbits of photons are obtained using the general method based on study of the effective potential and demonstrated with more details in Fig. 6.
- We also studied optical properties a black hole in Einstein-Æther gravity through light rays, that is a gravitational weak lensing. First, we focus on deflection angle around BH in Einstein-Æther gravity in the presence of plasma (uniform and non-uniform cases). In this part of our work, we have discussed and found that the influence of the uniform plasma on the deflection angle is greater than that in the non-uniform plasma case for fixed parameters of BH in Einstein-Æther gravity.
- Magnification of image is also explored using deflection angle of light rays, and it is shown with more details in Figs. 13 and 15.
- Finally, we investigated centre mass energy in vicinity BH with non-vanishing Einstein-Æther parameters c_{13} and c_{14}. We explored it for different values of the angular momentum of two particles and plotted the dependence of the energy of the centre of mass on the radial coordinate.

Acknowledgements F.A. acknowledges the support from Inha University in Tashkent, and research work has been supported by the Visitor Research Fellowship at Zhejiang Normal University. This work was partly supported by Grants F-FA-2021-432, F-FA-2021-510, and MRB-2021-527 of the Uzbekistan Ministry for Innovative Development and by the Abdus Salam International Centre for Theoretical Physics under the Grant No. OEA-NT-01. Research work of AA was supported by Chinese Academy of Science through PIFI fund.

References

1. C.M. Will, Living Rev. Relativ. **9**, 3 (2006). arXiv:gr-qc/0510072 [gr-qc]
2. B.P. Abbott et al., Phys. Rev. Lett. **116**, 061102 (2016). arXiv:1602.03837 [gr-qc]

3. K. Akiyama et al., ApJ **875**, L1 (2019). arXiv:1906.11238 [astro-ph.GA]
4. K. Akiyama et al., Astrophys. J. **875**, L6 (2019). arXiv:1906.11243 [astro-ph.GA]
5. M.A. Hohensee, N. Leefer, D. Budker, C. Harabati, V.A. Dzuba, V.V. Flambaum, Phys. Rev. Lett. **111**, 050401 (2013). arXiv:1303.2747 [hep-ph]
6. R. Aaij et al., Phys. Rev. Lett. **116**, 241601 (2016). arXiv:1603.04804 [hep-ex]
7. B. Zhang, J. Phys. B Atom. Mol. Phys. **53**, 235001 (2020). arXiv:2010.13590 [quant-ph]
8. C. Ding, A. Wang, X. Wang, Phys. Rev. D **92**, 084055 (2015a). arXiv:1507.06618 [gr-qc]
9. C. Zhang, X. Zhao, K. Lin, S. Zhang, W. Zhao, A. Wang, Phys. Rev. D **102**, 064043 (2020). arXiv:2004.06155 [gr-qc]
10. T. Zhu, Q. Wu, M. Jamil, K. Jusufi, Phys. Rev. D **100**, 044055 (2019). arXiv:1906.05673 [gr-qc]
11. M. Khodadi, E.N. Saridakis, Phys. Dark Universe **32**, 100835 (2021). arXiv:2012.05186 [gr-qc]
12. J. Oost, S. Mukohyama, A. Wang, Phys. Rev. D **97**, 124023 (2018). arXiv:1802.04303 [gr-qc]
13. M. Azreg-Aïnou, Z. Chen, B. Deng, M. Jamil, T. Zhu, Q. Wu, Y.-K. Lim, Phys. Rev. D **102**, 044028 (2020). arXiv:2004.02602 [gr-qc]
14. J. Rayimbaev, A. Abdujabbarov, M. Jamil, W.-B. Han, Nucl. Phys. B **966**, 115364 (2021). arXiv:2009.04898 [gr-qc]
15. B. Patla, R.J. Nemiroff, Astrophys. J. **685**, 1297 (2008). arXiv:0711.4811 [astro-ph]
16. Bozza, Phys. Rev. D **66**, 103001 (2002)
17. Bozza, S. Capozziello, G. Iovane, and G. Scarpetta, Gen. Rel. Grav. **33**, 1535 (2001)
18. E.P.E.S.E. Vázquez, Nuovo Cim. B **119**, 489 (2004)
19. G.S. Bisnovatyi-Kogan, O.Y. Tsupko, Astrophysics **51**, 99 (2008)
20. P. Schneider, J. Ehlers, E. Falco, *Gravitational Lenses. Astronomy and Astrophysics Library* (Springer, 1999). ISSN 0941-7834
21. V. Perlick, *Ray Optics, Fermat's Principle, and Applications to General Relativity* (Springer, Berlin, 2000)
22. V. Perlick, Liv. Rev. Relativ. **7**, 9 (2004)
23. J. Wambsganss, Liv. Rev. Relativ. **1**, 12 (1998). arXiv:astro-ph/9812021 [astro-ph]
24. K. Beckwith, C. Done, Mon. Not. R. Astron. Soc. **359**, 1217 (2005). arXiv:astro-ph/0411339 [astro-ph]
25. P.V.P. Cunha, C.A.R. Herdeiro, Gen. Relativ. Gravit. **50**, 42 (2018). arXiv:1801.00860 [gr-qc]
26. B. Narzilloev, S. Shaymatov, I. Hussain, A. Abdujabbarov, B. Ahmedov, C. Bambi, Eur. Phys. J. C **81**, 849 (2021a). arXiv:2109.02816 [gr-qc]
27. K.S. Virbhadra, C.R. Keeton, Phys. Rev. D **77**, 124014 (2008). arXiv:0710.2333 [gr-qc]
28. X. Pang, J. Jia, Class. Quantum Gravity **36**, 065012 (2019). arXiv:1806.04719 [gr-qc]
29. R. Kumar, S.U. Islam, S.G. Ghosh, Eur. Phys. J. C **80**, 1128 (2020). arXiv:2004.12970 [gr-qc]
30. Z. Li, G. Zhang, A. Övgün, Phys. Rev. D **101**, 124058 (2020). arXiv:2006.13047 [gr-qc]
31. A. Abdujabbarov, B. Ahmedov, N. Dadhich, F. Atamurotov, Phys. Rev. D **96**, 084017 (2017)
32. H. Sotani, U. Miyamoto, Phys. Rev. D **92**, 044052 (2015)
33. S.U. Islam, R. Kumara, S.G. Ghosha, J. Cosmol. A. P **2020**, 030 (2020)
34. S. Chakraborty, S. Soumitra, J. Cosmol. A. P. **07**, 045 (2017)
35. G.S. Bisnovatyi-Kogan, O.Y. Tsupko, Mon. Not. R. Astron. Soc. **404**, 1790 (2010)
36. O.Y. Tsupko, G.S. Bisnovatyi-Kogan, Gravit. Cosmol. **15**, 184 (2009)
37. V. Morozova, B. Ahmedov, A. Tursunov, Astrophys. Space Sci. **346**, 513 (2013)
38. A. Hakimov, F. Atamurotov, Astrophys. Space Sci. **361**, 112 (2016)
39. X. Er, S. Mao, Mon. Not. R. Astron. Soc. **437**, 2180 (2014). arXiv:1310.5825 [astro-ph.CO]
40. G.Z. Babar, F. Atamurotov, A.Z. Babar, Phys. Dark Universe **32**, 100798 (2021)
41. F. Atamurotov, A. Abdujabbarov, W.-B. Han, Phys. Rev. D **104**, 084015 (2021a)
42. F. Atamurotov, K. Jusufi, M. Jamil, A. Abdujabbarov, M. Azreg-Aïnou, Phys. Rev. D **104**, 064053 (2021b). arXiv:2109.08150 [gr-qc]
43. G.Z. Babar, F. Atamurotov, S. Ul Islam, S.G. Ghosh, Phys. Rev. D **103**, 084057 (2021). arXiv:2104.00714 [gr-qc]
44. A. Abdujabbarov, B. Toshmatov, J. Schee, Z. Stuchlík, B. Ahmedov, Int. J. Mod. Phys. D **26**, 1741011–187 (2017)
45. C. Benavides-Gallego, A. Abdujabbarov, Bambi, Eur. Phys. J. C **78**, 694 (2018)
46. F. Atamurotov, S. Shaymatov, P. Sheoran, S. Siwach, JCAP **2021**, 045 (2021c). arXiv:2105.02214 [gr-qc]
47. A. Rogers, Mon. Not. R. Astron. Soc. **451**, 17 (2015)
48. B. Turimov, B. Ahmedov, A. Abdujabbarov, C. Bambi, Int. J. Mod. Phys. D. **28**, 2040013 (2019)
49. F. Atamurotov, A. Abdujabbarov, J. Rayimbaev, Eur. Phys. J. C **81**, 118 (2021d)
50. F. Atamurotov, F. Sarikulov, A. Abdujabbarov, B. Ahmedov, Eur. Phys. J. Plus **137**, 336 (2022a)
51. F. Atamurotov, F. Sarikulov, V. Khamidov, A. Abdujabbarov, Eur. Phys. J. Plus **137**, 567 (2022b)
52. J.M. Bardeen, in *Black Holes (Les Astres Occlus)*, pp. 215–239 (1973)
53. H. Falcke, F. Melia, E. Agol, ApJ **528**, L13 (2000). arXiv:astro-ph/9912263 [astro-ph]
54. Q. Li, Y. Zhu, T. Wang, Eur. Phys. J. C **82**, 2 (2022). arXiv:2102.00957 [gr-qc]
55. V. Perlick, O.Y. Tsupko, Phys. Rev. D **95**, 104003 (2017). arXiv:1702.08768 [gr-qc]
56. W. Javed, A. Hamza, A. Övgün, Universe **7**, 385 (2021). arXiv:2110.11397 [gr-qc]
57. V. Perlick, O.Y. Tsupko, G.S. Bisnovatyi-Kogan, Phys. Rev. D **92**, 104031 (2015). arXiv:1507.04217 [gr-qc]
58. U. Papnoi, F. Atamurotov, Phys. Dark Universe **35**, 100916 (2022). arXiv:2111.15523 [gr-qc]
59. F. Atamurotov, U. Papnoi, K. Jusufi, Class. Quantum Gravity **39**, 025014 (2022c). arXiv:2104.14898 [gr-qc]
60. F. Atamurotov, B. Ahmedov, A. Abdujabbarov, Phys. Rev. D **92**, 084005 (2015). arXiv:1507.08131 [gr-qc]
61. P.V.P. Cunha, C.A.R. Herdeiro, B. Kleihaus, J. Kunz, E. Radu, Phys. Lett. B **768**, 373 (2017). arXiv:1701.00079 [gr-qc]
62. A. Abdujabbarov, F. Atamurotov, Y. Kucukakca, B. Ahmedov, U. Camci, Astrophys. Space Sci. **344**, 429 (2013). arXiv:1212.4949 [physics.gen-ph]
63. F. Atamurotov, A. Abdujabbarov, B. Ahmedov, Phys. Rev. D **88**, 064004 (2013a)
64. F. Atamurotov, A. Abdujabbarov, B. Ahmedov, Astrophys. Space Sci. **348**, 179 (2013b)
65. U. Papnoi, F. Atamurotov, S.G. Ghosh, B. Ahmedov, Phys. Rev. D **90**, 024073 (2014). arXiv:1407.0834 [gr-qc]
66. F. Atamurotov, S.G. Ghosh, B. Ahmedov, Eur. Phys. J. C **76**, 273 (2016). arXiv:1506.03690 [gr-qc]
67. S.G. Ghosh, M. Amir, S.D. Maharaj, Nucl. Phys. B **957**, 115088 (2020)
68. J. Badía, E.F. Eiroa, Phys. Rev. D **104**, 084055 (2021). arXiv:2106.07601 [gr-qc]
69. K. Jafarzade, M. Kord Zangeneh, F. S. N. Lobo, J. Cosmol. A. P. **2021**, 008 (2021). arXiv:2010.05755 [gr-qc]
70. A. Chowdhuri, A. Bhattacharyya, Phys. Rev. D **104**, 064039 (2021). arXiv:2012.12914 [gr-qc]
71. M. Ghasemi-Nodehi, M. Azreg-Aïnou, K. Jusufi, M. Jamil, Phys. Rev. D **102**, 104032 (2020). arXiv:2011.02276 [gr-qc]
72. M. Afrin, R. Kumar, S.G. Ghosh, Mon. Not. R. Astron. Soc. **504**, 5927 (2021). arXiv:2103.11417 [gr-qc]
73. G.Z. Babar, A.Z. Babar, F. Atamurotov, Eur. Phys. J. C **80**, 761 (2020)

74. M. Bañados, J. Silk, S.M. West, Phys. Rev. Lett. **103**, 111102 (2009). arXiv:0909.0169 [hep-ph]
75. A. Jawad, F. Ali, M.U. Shahzad, G. Abbas, Eur. Phys. J. C **76**, 586 (2016). arXiv:1610.05610 [physics.gen-ph]
76. E. Teo, Gen. Relativ. Gravit. **35**, 1909 (2003)
77. O.B. Zaslavskii, Phys. Rev. D **85**, 024029 (2012). arXiv:1110.5838 [gr-qc]
78. B. Narzilloev, S. Shaymatov, I. Hussain, A. Abdujabbarov, B. Ahmedov, C. Bambi, Eur. Phys. J. C **81**, 849 (2021b). arXiv:2109.02816 [gr-qc]
79. B. Turimov, J. Rayimbaev, A. Abdujabbarov, B. Ahmedov, Z. Stuchlík, Phys. Rev. D **102**, 064052 (2020). arXiv:2008.08613 [gr-qc]
80. S.E. Gralla, A.P. Porfyriadis, N. Warburton, Phys. Rev. D **92**, 064029 (2015). arXiv:1506.08496 [gr-qc]
81. P.I. Jefremov, O.Y. Tsupko, G.S. Bisnovatyi-Kogan, Phys. Rev. D **91**, 124030 (2015). arXiv:1503.07060 [gr-qc]
82. C. Chakraborty, S. Bhattacharyya, JCAP **2019**, 034 (2019). arXiv:1901.04233 [astro-ph.HE]
83. S. Shaymatov, F. Atamurotov, Galaxies **9**, 40 (2021). arXiv:2007.10793 [gr-qc]
84. F. Atamurotov, S. Shaymatov, B. Ahmedov, Galaxies **9**, 54 (2021e)
85. E. Hackmann, H. Nandan, P. Sheoran, Phys. Lett. B **810**, 135850 135850 (2020). arXiv:2006.05045 [gr-qc]
86. A. Abdujabbarov, B. Ahmedov, B. Ahmedov, Phys. Rev. D **84**, 044044 (2011). arXiv:1107.5389 [astro-ph.SR]
87. A.H. Bokhari, J. Rayimbaev, B. Ahmedov, Phys. Rev. D **102**, 124078 (2020)
88. B. Narzilloev, J. Rayimbaev, S. Shaymatov, A. Abdujabbarov, B. Ahmedov, C. Bambi, Phys. Rev. D **102**, 104062 (2020). arXiv:2011.06148 [gr-qc]
89. Z. Stuchlík, M. Blaschke, J. Schee, Phys. Rev. D **96**, 104050 (2017). arXiv:1711.10890 [gr-qc]
90. B. Toshmatov, A. Abdujabbarov, B. Ahmedov, Z. Stuchlík, Astrophys. Space Sci. **357**, 41 (2015). arXiv:1407.3697 [gr-qc]
91. A. Abdujabbarov, F. Atamurotov, N. Dadhich, B. Ahmedov, Z. Stuchlík, Eur. Phys. J. C **75**, 399 (2015)
92. T. Jacobson, D. Mattingly, Phys. Rev. D **64**, 024028 (2001). arXiv:gr-qc/0007031 [gr-qc]
93. B.Z. Foster, Phys. Rev. D **75**, 129904 (2007)
94. D. Garfinkle, C. Eling, T. Jacobson, Phys. Rev. D **76**, 024003 (2007). arXiv:gr-qc/0703093 [gr-qc]
95. C. Ding, A. Wang, X. Wang, Phys. Rev. D **92**, 084055 (2015b). arXiv:1507.06618 [gr-qc]